Anbar Journal Of Engineering Science©

journal homepage: http:// http://www.uoanbar.edu.iq/Evaluate/

Unviersty of Anbar

Static analysis of two-directional functionally graded cylindrical panels under the effect of symmetric loads using finite element method (FEM)

Qutaibah M. Mohammed [a*], Hamad M. Hasan [b]

[a] *An engineer in the Directorate of Water Resources in Anbar, State Commission On Operation of Irrigation and Drainage Projects, Ministry of Water Resources, Ramadi, Anbar, Iraq*

[b] *Department of Mechanical Engineering, Faculty of Engineering, Anbar University, Ministry of Higher Education & Scientific Research, Ramadi, Anbar, Iraq*

PAPER INFO

Paper history:
Received … … …
Received in revised form … … …
Accepted … … …

Keywords:
Static analysis
Two directional functionally graded cylindrical panels
First-order shear deformation theory
Linear analysis
Finite element method

ABSTRACT

This paper offers the linear analysis of the static behavior of two directional functionally graded (2D-FG) cylindrical panels under the effect of internal symmetric loads. The mechanical properties of the cylindrical panel are given to be changed simultaneously through the thickness and longitudinal directions as a function to the volume fraction of the constituents by a simple power-law distribution. Based on Sander's first order shear deformation shell theory (FSDT), the equations of motion for (2D-FG) panels are derived using the principle of minimum total potential energy (MPE). The finite element method (FEM) as an effective numerical tool is utilized to solve the equations of motion. The model has been compared with those available in the literature and it observed good correspondence. The influences of the material variation along the thickness and longitudinal directions, geometrical parameters, boundary conditions and load parameters on the panel deformation are studied in detail.

1. Introduction

The first presentation of functionally graded materials (FGMs) was used in Japan in the year 1984 by a group of the material scientists and the attention of researchers has concentrated frequently in this type of materials [1]. FGMs are new types of sophisticated heterogeneous composite materials in which their material properties are characterized by a sleek and uninterrupted variation simultaneously along one (or more) direction(s) [2]. The mixture from ceramics and metals are generally used in manufacturing FGMs to fulfill the requirements in a variety engineering locations for survivorship in severe environments (high mechanical and thermal loadings) [3]. To control carefully the deformations and stresses, 2-D FG plates may be used in most engineering applications. Some researchers studied the deformations of 2-D FG circular and rectangular and square plates subjected to various loadings. Under the effect of thermal loading, the elastic-plastic deformations of 2-D FGMs were investigated by Nemat *et al.* [4]. 2-D FG circular and annular plates subjected to axisymmetric bending are studied by Nie and Zhong [5]. Asemi *et al.* [6] calculated the deformations of fully clamped 2-D FG square plates using 3-D elasticity theory and FEM. Alinaghizadeh and Shariati [7] used generalized differential quadrature method (GDQM) to study linear and nonlinear deflection of thick 2-D FG annular sector and rectangular plates using FSDT and HSDT9.

Cylindrical shells and panels in structural components play a major role in engineering applications. The idea of FGMs avoids sudden changes in the stress and displacement distributions during thickness of the shell and panel structures. Several researchers have been presented to study the static behavior of FG cylindrical shells and panels as [8-20]. The extension and flexure of cylindrical and spherical thin elastic shells are presented by general survey from Basset [8]. Horgan and Chan [9] calculated the deformations of a FG cylinder using power-law function between elastic modulus and radius with constant Poisson's ratio. Under the effect of combined axial and radial mechanical loads, post buckling demeanor of FG cylindrical shells in high-temperature state is studied by Shen and Noda [10]. Zhao *et al.* [11] determined static deflection of FG cylindrical shells under the effect of symmetric loads. The influences of power-law distribution of continuously graded fiber rein-forced cylindrical shells using 3-D analysis of thermal stresses are discussed by Aragh and Yas [12,13]. The static deformations of FG cylindrical shell bonded to thin piezoelectric layers were calculated by Alibeigloo [14] using thermo-elastic solutions. By using DQM, the static analysis of FG cylindrical shells with piezoelectric layers are presented by Alibeigloo and Nouri [15]. Liew *et al.* [16] presented analysis of the thermal stress behavior of FG hollow circular cylinders. Viola *et al.* [17,18] used generalized unconstrained third order theory to study static analysis of FG cylindrical, conical shells and panels. Under the effect of compression loading, the deformations of moderately thick FG conical panels are estimated by Aghdam *et al.* [19]. FG conical shells with stress and displacement recovery were investigated by Rosseti *et al.* [20]. In complex design problems, 1-D FG cylindrical shell and panel may also not be so effective because all their outer surfaces will have the same synthesis and heat allocation. Therefore, shell and panel elements in advanced machine are preferred to change in properties in two or three directions to give more efficiency to the structures and reduce the deformations and stresses. Nemat-Alla [21] submitted the conception of appending a third material to (FGMs) to resist the dangerous thermal stresses. Aragh and Hedayati [22] calculated the effect of natural frequency parameters on 2-D FG cylindrical shells using (GDQM). The natural frequency effect on cylindrical shells are made from 2-D FG ceramic/metal is determined by Ebrahimi and Najafizadeh [23] using GDQM. The influence of 2-D material distribution on the dynamic demeanor of thick finite length cylinder structure and the thermal stress distributions were presented by Asgari and Akhlaghi [24]. Najibi and Talebitooti [25] studied nonlinear transient thermo-elastic analysis a two-dimensional FG thick hollow finite length cylinder under effect of thermal loading using (FEM). Literature survey showed that most treatises on cylindrical shells and panels are restricted to conventional FG cylindrical shells and panels, so this work may be exercised as a beneficial research for recipient studies. In the present work, linear analysis of 2-D FG cylindrical panels is studied using (FEM) method jointly with (FSDT). The material distribution is given to be changed simultaneously through thickness and longitudinal directions as a simple power-law distribution. To confirm the accuracy and validity of results, a comparison study is performed.

2. Geometry of model and material distribution

Assuming a 2-D FG cylindrical panel of length a, radius R, span angle θ_0, span length b = R θ_0, and uniform thickness h, where the origin of a coordinate system (x, y, z) is a group at the mid-plane of the panel as shown in Fig. 1. This panel is made from four different constituent materials whose properties P are changed simultaneously in two directions (z, x) during thickness and longitudinal directions as a function of the volume fraction and material properties [7].

$$PR\left(z\,,\,x\right)=PR_{c1}V_{c1}+PR_{c2}V_{c2}+PR_{m1}V_{m1}+PR_{m2}V_{m2} \quad (1)$$

Where PR refer to the effective material properties, such as Young's modulus E and other physical properties except for the Poisson's ratio is considered 0.3 in the present work.

The subscripts c1 and c2 denote to first and second ceramic while m1 and m2 first and second metal constituents and V_{ij} (i = c, m and j = 1, 2) represents volume fraction of the material constituents ij which can be described by a power-law distribution as [7]:

$$V_{c1}=\left[1-\left(\frac{x}{a}\right)^{nx}\right]\left(\frac{z}{h}+\frac{1}{2}\right)^{nz} \quad (2a)$$

$$V_{c2}=\left(\frac{x}{a}\right)^{nx}\ \left(\frac{z}{h}+\frac{1}{2}\right)^{nz} \quad (2b)$$

$$V_{m1}=\left[1-\left(\frac{x}{a}\right)^{nx}\right]\ \left[1-\left(\frac{z}{h}+\frac{1}{2}\right)^{nz}\right] \quad (2c)$$

$$V_{m2}=\left(\frac{x}{a}\right)^{nx}\left[1-\left(\frac{z}{h}+\frac{1}{2}\right)^{nz}\right] \quad (2d)$$

Where nx and nz represent power law indices through thickness and longitudinal directions; respectively. By substituting Eq. (2) into Eq. (1)

Young's modulus property E(z, x) can be explained as:

$$E(z,x) = \left[E_{m1} + (E_{m2} - E_{m1})\left(\frac{x}{a}\right)^{nx}\right]\left[1 - \left(\frac{z}{h} + \frac{1}{2}\right)^{nz}\right] + \left[E_{c1} + (E_{c2} - E_{c1})\left(\frac{x}{a}\right)^{nx}\right]\left(\frac{z}{h} + \frac{1}{2}\right)^{nz} \quad (3)$$

It can be seen from Eq. (3) that the lower and upper edges at (x, y, z) = (0, y, h/2),(0, y, -h/2),(a, y, h/2),(a, y, -h/2) represent first ceramic, first metal, second ceramic, second metal; respectively, as it is observed in Fig. 1. The magnitudes of power- law indices are (∞ ≥ (nx, nz) ≥ 0).

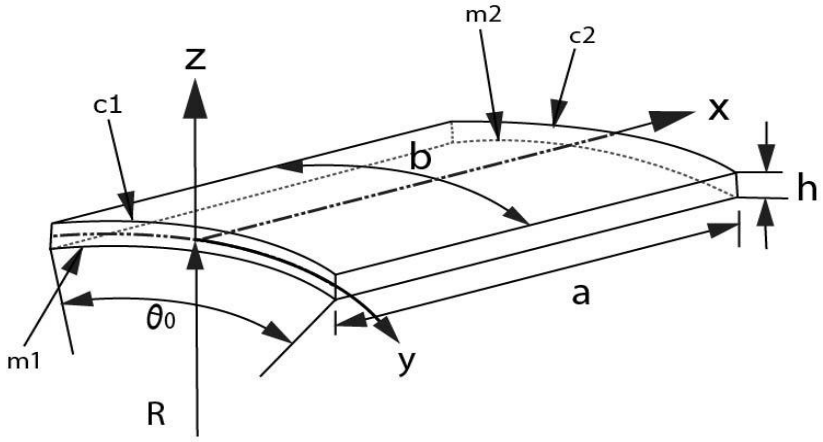

Figure 1. The model geometry of a two-directional FG cylindrical panel.

3. Theoretical formulation

3.1. Displacement field and strains

In this paper, the equations of motion for 2-D FG panel are derived by using minimum potential energy (MPE). The in-plane displacements u, v and the transverse displacement w for the panel are given by using Sander's first order shear deformation theory (FSDT) [26]:

$$u(x,y,z) = \boldsymbol{u_0}(x,y) + z\,\boldsymbol{\varphi_x}(x,y) \quad (4a)$$

$$v(x,y,z) = \boldsymbol{v_0}(x,y) + z\,\boldsymbol{\varphi_y}(x,y) \quad (4b)$$

$$w(x,y,z) = \boldsymbol{w_0}(x,y) \quad (4c)$$

where u, v and w represent the displacements of a point along the (x, y, z) coordinates. u_0, v_0 and w_0 are the displacements of a point on the mid-plane. $\boldsymbol{\varphi_x}$ and $\boldsymbol{\varphi_y}$ are the rotations of normal to the mid-plane about the y-axis and x-axis, respectively.

The linear strain components are calculated by substitution Eqs. (4) into linear strain-displacement relations as follows [29]:

$$\boldsymbol{\varepsilon_{xx}} = \frac{\partial \boldsymbol{u_0}}{\partial \boldsymbol{x}} + \boldsymbol{z}\frac{\partial \boldsymbol{\varphi_x}}{\partial \boldsymbol{x}} \quad (5a)$$

$$\boldsymbol{\varepsilon_{yy}} = \frac{\partial \boldsymbol{v_0}}{\partial \boldsymbol{y}} + \boldsymbol{z}\frac{\partial \boldsymbol{\varphi_y}}{\partial \boldsymbol{y}} + \frac{\boldsymbol{w_0}}{\boldsymbol{R}} \quad (5b)$$

$$\boldsymbol{\gamma_{xy}} = \frac{\partial \boldsymbol{u_0}}{\partial \boldsymbol{y}} + \frac{\partial \boldsymbol{v_0}}{\partial \boldsymbol{x}} + \boldsymbol{z}\frac{\partial \boldsymbol{\varphi_x}}{\partial \boldsymbol{y}} + \boldsymbol{z}\frac{\partial \boldsymbol{\varphi_y}}{\partial \boldsymbol{x}} \quad (5c)$$

$$\boldsymbol{\gamma_{yz}} = \boldsymbol{\varphi_y} + \frac{\partial \boldsymbol{w_0}}{\partial \boldsymbol{y}} - \frac{\boldsymbol{v_0}}{\boldsymbol{R}} \quad (5d)$$

$$\boldsymbol{\gamma_{xz}} = \boldsymbol{\varphi_x} + \frac{\partial \boldsymbol{w_0}}{\partial \boldsymbol{x}} \quad (5e)$$

3.2. Constitutive relations

By assuming the plane-stress state, the linear stress-strains relation will be obtained as follows [29]:

$$\sigma_{xx} = \left[\frac{E(z,x)}{(1-\nu^2)}\right](\varepsilon_{xx} + \nu\varepsilon_{yy}) \quad (6a)$$

$$\sigma_{yy} = \left[\frac{E(z,x)}{(1-\nu^2)}\right](\varepsilon_{yy} + \nu\,\varepsilon_{xx}) \quad (6b)$$

$$\boldsymbol{\sigma_{xy}} = \left[\frac{E(z,x)}{2(1+\nu)}\right] (\boldsymbol{\gamma_{xy}}) \quad (6c)$$

$$\boldsymbol{\sigma_{yz}} = k_s \left[\frac{E(z,x)}{2(1+\nu)}\right] (\boldsymbol{\gamma_{yz}}) \quad (6d)$$

$$\boldsymbol{\sigma_{xz}} = k_s \left[\frac{E(z,x)}{2(1+\nu)}\right] (\boldsymbol{\gamma_{xz}}) \quad (6e)$$

Where k_s is the shear correction factor taken to be 5/6.

3.3. Strain energy

The strain energy of the 2-D FG cylindrical panel is expressed as [28]:

$$U = \left(\frac{1}{2}\right) {}_{Vol}\int \{\varepsilon_{ij}\}^T \{\boldsymbol{\sigma}_{ij}\}\, dV \quad (7)$$

Where ε_{ij} and $\boldsymbol{\sigma}_{ij}$ (i, j=x, y, z) are the strain and stress tensor components.

3.4. Work done due to transverse load

The panel under the effect of symmetric load P_0, work done on the panel may be expressed as [28]:

$$W = \left(\frac{1}{2}\right) {}_{A}\int \boldsymbol{P_0}(x, y)\{w_0\}\, dA \quad (8)$$

4. Solution methodology

4.1. Finite element modeling

As aforementioned in this study, the (FEM) is utilized to solve the equations of motion in the locative field. In the state of symmetric loading, one has two-dimensional problems and so those appropriate two-dimensional elements should be chosen to describe the 2-D FG cylindrical panels. In the present work, a four-node isoparametric rectangular element and five degrees of freedom per node are utilized for finite element styling. The range in the finite element is described into a group of finite rectangular elements, any of the elements has the displacement vector and element geometry of the style is explained by [27]:

$$\{d\} = \sum_{i=1}^{NPE} Ni\, \{d\}i, \qquad x = \sum_{i=1}^{NPE} Ni\, xi, \quad y = \sum_{i=1}^{NPE} Ni\, yi \quad (9)$$

Where Ni denotes the interpolation function (shape function) for the ith node, $\{d\}$i represents the vector of unknown displacements for the ith node, NPE is the number of nodes per element and xi and yi are Cartesian coordinate of the ith node. The interpolation functions which are employed to the finite element estimation are expressed by [27]:

$$N_1 = 0.25(1-\xi)(1-\eta) \quad (10a)$$

$$N_2 = 0.25(1+\xi)(1-\eta) \quad (10b)$$

$$N_3 = 0.25(1+\xi)(1+\eta) \quad (10c)$$

$$N_4 = 0.25(1-\xi)(1+\eta) \quad (10d)$$

4.2. Governing equation

The governing equation for static analysis of 2-D FG panel can be derived utilizing the principle of minimum total potential energy (MPE). The equations of motion of the typical element "e" according to principle of (MPE) can be expressed as [28]:

$$\delta U^{(e)} - \delta W^{(e)} = 0 \quad (11)$$

Where $\delta U^{(e)}$ and $\delta W^{(e)}$ are the variations of the potential energy of the eth element and virtual work done of the external symmetric load on the eth element. Next to, a coordinating (e) is employed to indicate the physical and geometrical parameters of the eth element.

Based on the FSDT and from Eq. (7), the variation of the potential energy of the eth element can be expressed as [28]:

$$\boldsymbol{\delta U^{(e)}} = \int_{A^{(e)}} \int_{\frac{-h}{2}}^{\frac{h}{2}} \left[\boldsymbol{\sigma_{xx}^{(e)}\delta\varepsilon_{xx}^{(e)}} + \boldsymbol{\sigma_{yy}^{(e)}\delta\varepsilon_{yy}^{(e)}} + \boldsymbol{\sigma_{xy}^{(e)}\delta\gamma_{xy}^{(e)}} + \boldsymbol{\sigma_{yz}^{(e)}\delta\gamma_{yz}^{(e)}} + \boldsymbol{\sigma_{xz}^{(e)}\delta\gamma_{xz}^{(e)}}\right] \boldsymbol{dz dA} \quad (12)$$

From Eq. (8), the virtual work done due to uniform load on the eth element can be expressed as [28]:

$$\boldsymbol{\delta W^{(e)}} = \int_{A^{(e)}} \boldsymbol{P_0^{(e)}}\{\boldsymbol{\delta w_0^{(e)}}\}\boldsymbol{dA} \quad (13)$$

Where $A^{(e)}$ is the eth element area.

The governing equations of motion for linear static analysis with small deformation of the eth 2-D FG panel element can be obtained by substituting Eqs. (12) and (13) into Eq. (11) as follows [27]:

$$[K^{(e)}]\{d^{(e)}\} = \{F^{(e)}\} \quad (14)$$

Where $[K^{(e)}]$, $\{d^{(e)}\}$ and $\{F^{(e)}\}$ are the linear stiffness matrix, vector of degrees of freedom and force vector of the eth element; respectively [27].

$$[K^{(e)}] = \begin{bmatrix} \boldsymbol{K_{11}^{(e)}} & \boldsymbol{K_{12}^{(e)}} & \boldsymbol{K_{13}^{(e)}} & \boldsymbol{K_{14}^{(e)}} & \boldsymbol{K_{15}^{(e)}} \\ \boldsymbol{K_{21}^{(e)}} & \boldsymbol{K_{22}^{(e)}} & \boldsymbol{K_{23}^{(e)}} & \boldsymbol{K_{24}^{(e)}} & \boldsymbol{K_{25}^{(e)}} \\ \boldsymbol{K_{31}^{(e)}} & \boldsymbol{K_{32}^{(e)}} & \boldsymbol{K_{33}^{(e)}} & \boldsymbol{K_{34}^{(e)}} & \boldsymbol{K_{35}^{(e)}} \\ \boldsymbol{K_{41}^{(e)}} & \boldsymbol{K_{42}^{(e)}} & \boldsymbol{K_{43}^{(e)}} & \boldsymbol{K_{44}^{(e)}} & \boldsymbol{K_{45}^{(e)}} \\ \boldsymbol{K_{51}^{(e)}} & \boldsymbol{K_{52}^{(e)}} & \boldsymbol{K_{53}^{(e)}} & \boldsymbol{K_{54}^{(e)}} & \boldsymbol{K_{55}^{(e)}} \end{bmatrix}$$

$$\{F^{(e)}\} = \begin{Bmatrix} F_1^{(e)} \\ F_2^{(e)} \\ F_3^{(e)} \\ F_4^{(e)} \\ F_5^{(e)} \end{Bmatrix} \quad \{d^{(e)}\} = \begin{Bmatrix} u_0^{(e)} \\ v_0^{(e)} \\ w_0^{(e)} \\ \varphi_x^{(e)} \\ \varphi_y^{(e)} \end{Bmatrix} \tag{15}$$

After assembling the element stiffness matrix [K(e)] and element load vector {F(e)} will be obtained on the global stiffness matrix [K] and global load vector {F} as [27]:

$$[K]\{d\} = \{F\} \tag{16}$$

5. Numerical results

The linear analysis of 2-D FG panel are calculated using the principle of (MPE) in conjunction with (FEM). A computer program has been advanced in FORTRAN Plato IDE (FTN95) environment. In this study, various boundary conditions are employed to improve the effectiveness of present method. Table. 1 shows the properties of 2-D FG panel constituents given at room temperature (27°c), which have been employed to calculate the results of the present work.

Table 1. The Young's modulus property for metals and ceramics constituents of 2-D FG panel

Materials	Young's modulus
Tie6Ale4V	E_{m1}=105.7GPa
Aluminum (Al)	E_{m2}=70GPa
Alumina (Al2O3)	E_{c1}=380GPa
Zirconia (ZrO2)	E_{c2}=151GPa

It is assumed that the deformation of the panel is within the elastic limits. The boundary conditions used in the present study are as follows:

Clamped (CCCC): $u_0 = v_0 = w_0 = \varphi_x = \varphi_y = 0$, at x = 0, a and y = b/2, -b/2.

Simply supported (SSSS): $v_0 = w_0 = \varphi_y = 0$, at x = 0, a and $u_0 = w_0 = \varphi_x = 0$, at y = b/2, –b/2.

Clamped-Simply supported (CSCS): $u_0 = v_0 = w_0 = \varphi_x = \varphi_y = 0$, at y = b/2, -b/2 and $v_0 = w_0 = \varphi_y = 0$, at x = 0, a.

Simply supported-clamped (SCSC): $u_0 = v_0 = w_0 = \varphi_x = \varphi_y = 0$, at x = 0, a and $u_0 = w_0 = \varphi_x = 0$, at y = b/2, – b/2.

5.1. Convergence tests

It is aforementioned that the precision of the present method is dependent on a number of elements along longitudinal (N_x) and circumferential (N_y). Convergence studies are first accomplished to appoint the prerequisite number of elements in longitudinal and circumferential directions, as N_x and N_y, respectively. Fig. 2 shows convergence test of dimensionless deflections at the center point (x, y) = (a/2, 0) of 2-D FG cylindrical panels with different boundary conditions based on FSDT for (load = 1MPa, a = 0.2, b = 0.2, h = 0.01, R = 1, nx = 1, nz = 1). Fig. 2 shows the convergence of the method is obtained between (60*60) and (70*70) mesh size for all the boundary conditions, the mesh size (60*60) are sufficient to achieve converged results.

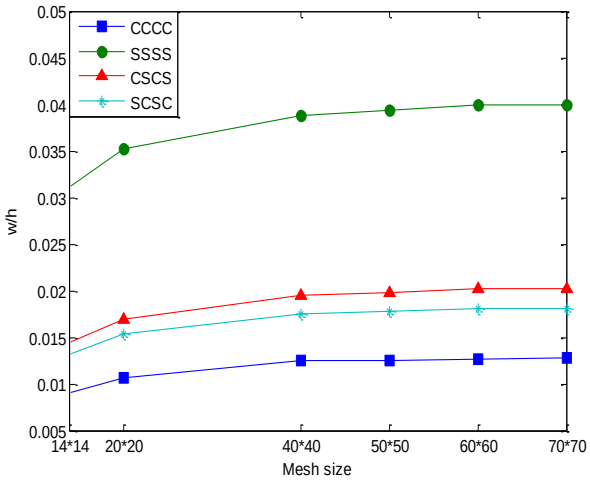

Figure 2. Convergence test of present results for dimensionless center deflections of 2-D FG cylinderical panels with different boundary conditions for (nx , nz)= (1 , 1).

5.2. Comparison studies

To check the reliability and proficiency of present method, two test cases for comparison studies are accomplished. As the first test, 1-D FG square panel with fully clamped and simply supported edges (a*b) = (0.2*0.2) subjected to uniform load = 1MPa for (R = 1, h = 0.01, nx = 0, nz = 0,1,5) are considered. FSDT is used to predict the results for dimensionless center deflections of 1-D FG (Al/ZrO_2) square panel with different mesh sizes are given in Table 2 and are contrasted with those adduced by Viola *et al.* [20]. Moreover, anticipation's present results for non-dimensional center deflections are slightly smaller than those of FSDT with percentage difference between (1.03% - 1.7%).

To validate the present methodology in the state of 2-D FG structures, another comparison study with 2-D FG square plates is completed. Geometry of a cylindrical panel may guide to a square plate with sides (a*a) by assuming the following infinitely radius and very small angle (R = ∞, θ0 = 0o).

Table 2. Comparison of the dimensionless center deflection (**Al/ZrO2**) square shell for various volume fraction index (nz) and nx = 0 and R/h = 100 with different mesh size.

Mesh size	**(w/h) at center CCCC Volume fraction index (nz)**			**(w/h) at center SSSS Volume fraction index (nz)**		
	0	**1**	**5**	**0**	**1**	**5**
14*14	0.009898	0.0139	0.01714	0.0339	0.04784	0.05827
20*20	0.01154	0.0163	0.01983	0.0379142	0.053716	0.06478
40*40	0.013127	0.01863	0.0224	0.04145	0.058926	0.070442
50*50	0.013348	0.01896	0.022734	0.041914	0.05962	0.0712
60*60	0.01357	0.01927	0.0231	0.0425	0.060426	0.07212
70*70	0.013594	0.01931	0.02313	0.04248	0.060488	0.0721
Ref.[20] (FSDT)	0.013831	0.01964	0.023488	0.042991	0.06114	0.07285
Percentage difference	1.7%	1.7%	1.5%	1.2%	1.1%	1.03%

Fig. 3 shows comparisons of the present method results with other different methods for change of deflection during longitudinal middle line (x, y) = (x, a/2) of thick 2-D FG square plates (a*b) = (1*1) and h = 0.4 with fully clamped edges under the effect of symmetric pressure PZ = 40 MPa. At the edges of plate (0, y, h/2), (0, y, -h/2), (a, y, h/2) and (a, y, -h/2), Young's modulus is assumed to be 115GPa, 440GPa, 69GPa and 300GPa; respectively, and Poisson's ratio is assumed a constant value of 0.3. Logically excellent correspondence can be seen between present results and those obtained in accordance with the 3-D elasticity theory using FEM [6] and HSDT9, FSDT using GDQ [7]. Also, the model of HSDT9 predicts actual transverse shear deformation in such thick plates higher than FSDT. Consequently, the difference between results of the FSDT and 3-D elasticity theory is higher than of the HSDT9. So, it can be seen that the predictions of FSDT for deflections are higher than the HSDT9.

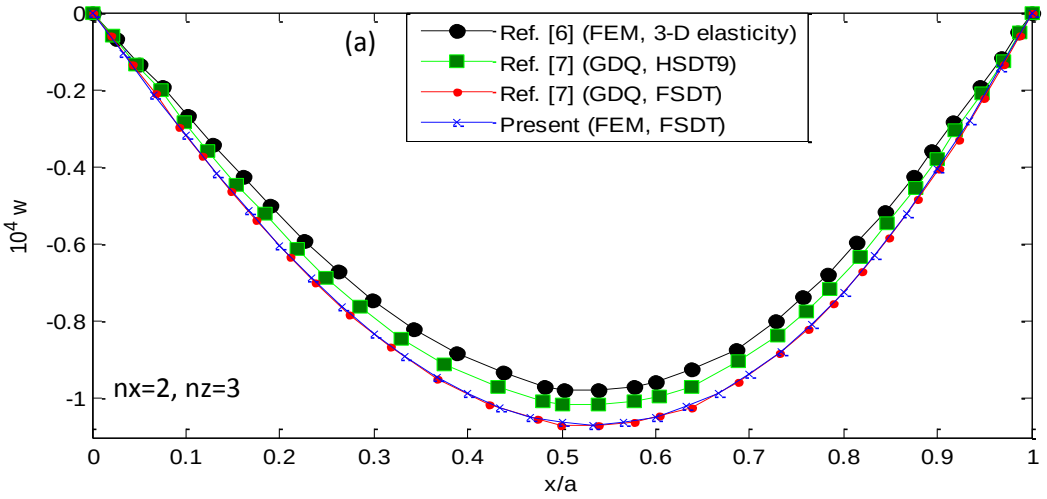

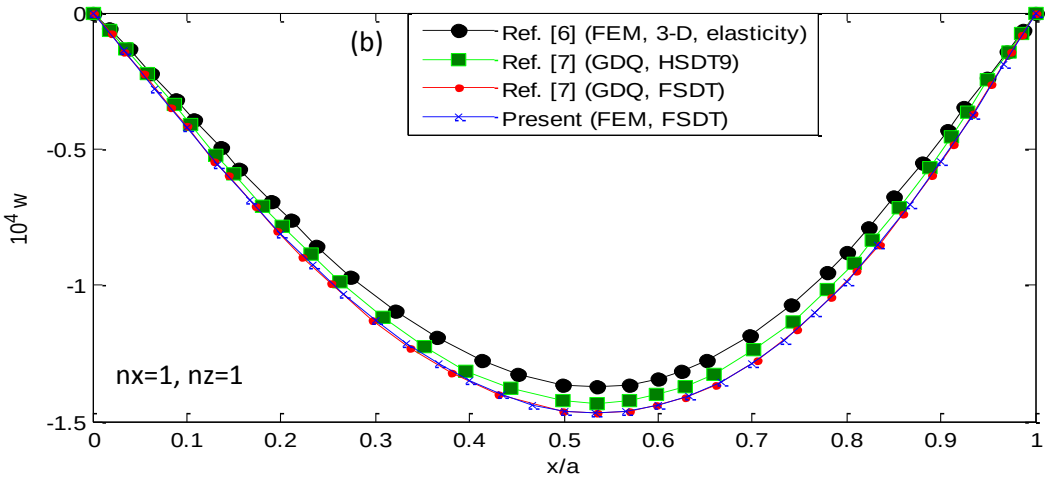

Figure 3. (a)-(b) Comparisons of the present method results with other different methods for change of deflection along middle line (x, a/2) of thick fully clamped 2-D FG square plates.

6. Results and discussion

It is mentioned above that the (60*60) mesh size has been found to give good convergence for the 2-D FG cylindrical panels. These have been utilized for perfecting the results, except if another way declared. In the present work, Poisson's ratio is assumed to be constant and equal to 0.3 in all computations. Effects of material distribution on the change of dimensionless deflection during longitudinal middle line (x, 0) of the (CCCC, SSSS, CSCS, SCSC) cylindrical panels for various magnitudes of the power-law indices nx and nz are shown in Figs. 4, 5, 6 and 7; respectively. The deflections are computed for panels are assumed to be under uniform load $P_z a^4/E_{m2}h^4 = 2.285715$ and (R = 1, $\theta_0 = 11.46^o$). As it can be seen in Figs. (4, 5, 6 and 7), both value and model of the deflections rely on the magnitudes of the power-law indices. By increasing magnitudes of nz with a constant value of nx, deflection of the panels increases as the volume fractions of ceramics (i.e., alumina and zirconia) and stiffness decrease. Moreover, by increasing the magnitudes of nx with a constant value of nz, maximum deflection position changes because of the variation in material distribution during longitudinal direction.

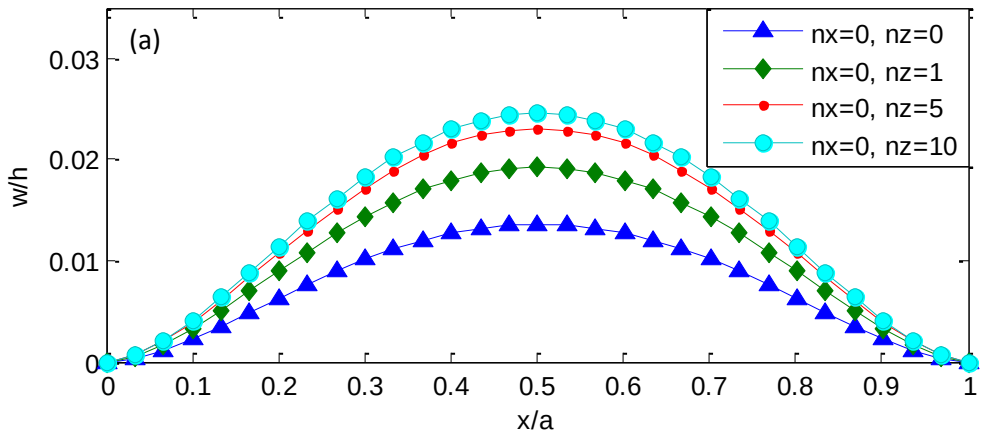

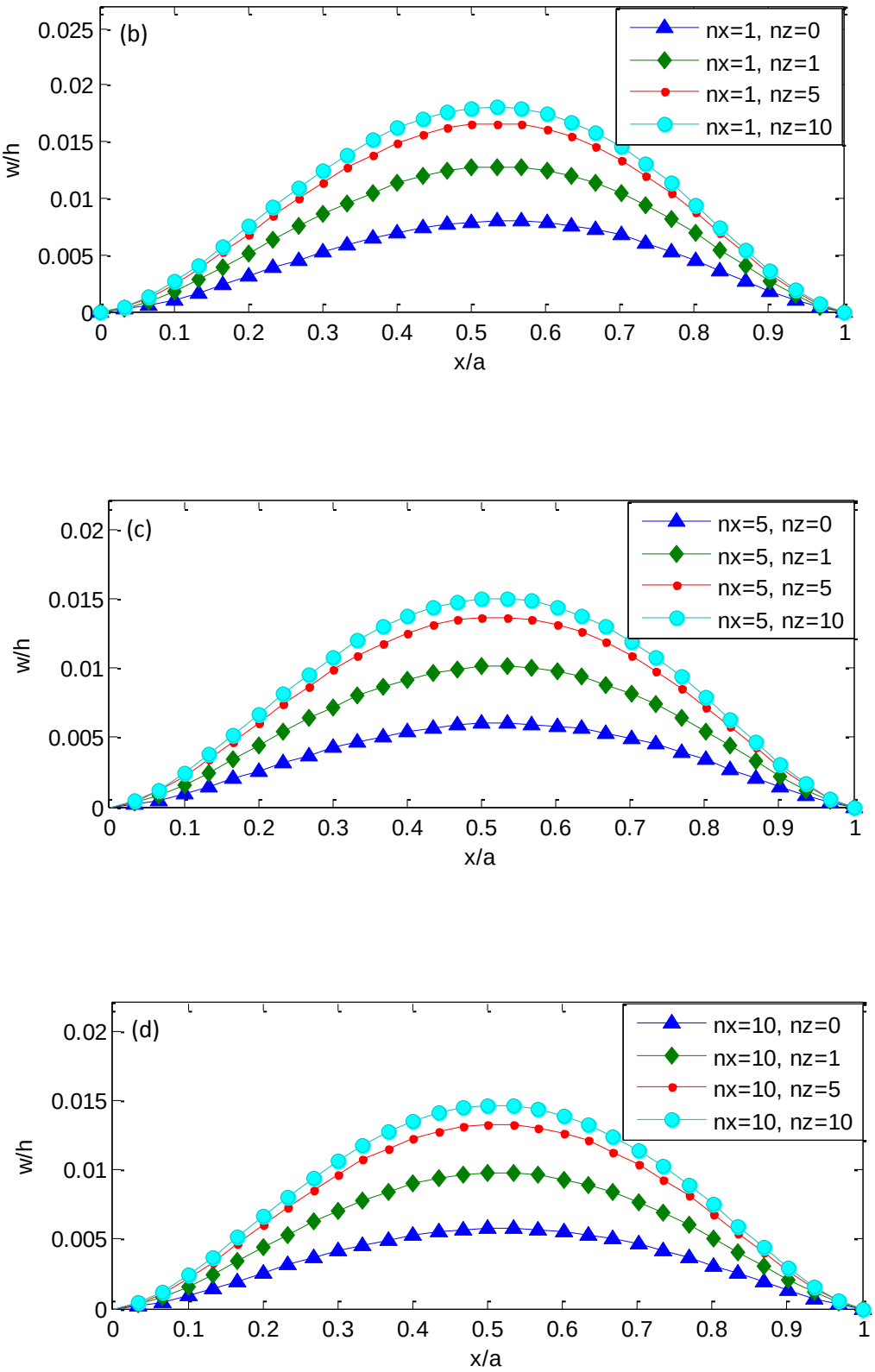

Figure 4. (a)-(d) Effects of material distribution on the change of dimensionless deflection during longitudinal middle line of fully clamped cylindrical panels with various magnitudes of the power-law indices.

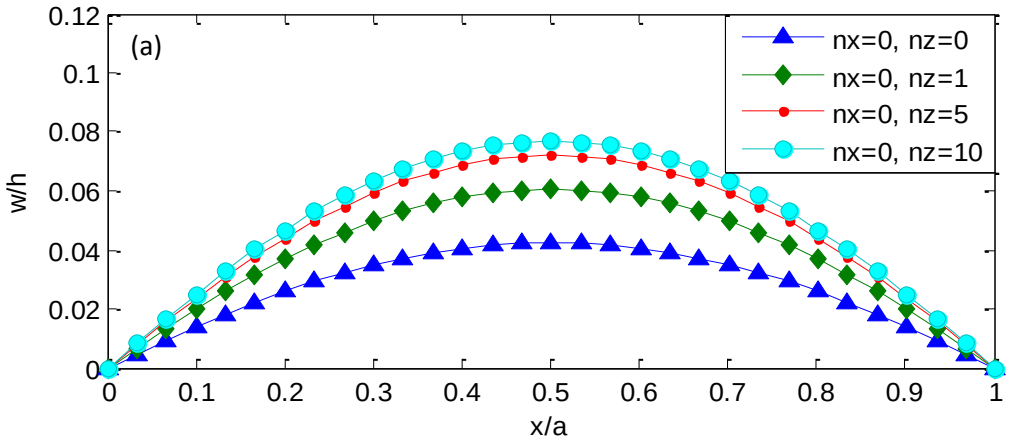
(a)
nx=0, nz=0
nx=0, nz=1
nx=0, nz=5
nx=0, nz=10
w/h
x/a
0.12
0.1
0.08
0.06
0.04
0.02
0
0.1
0.2
0.3
0.4
0.5
0.6
0.7
0.8
0.9
1

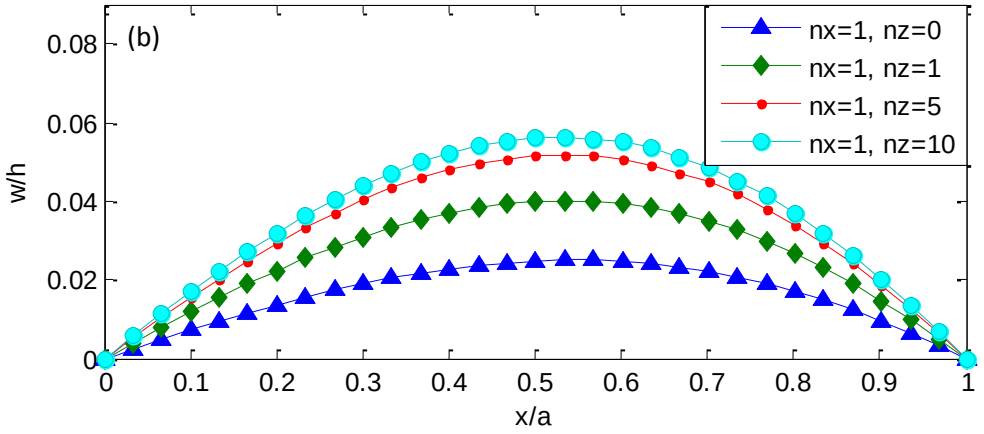
(b)
nx=1, nz=0
nx=1, nz=1
nx=1, nz=5
nx=1, nz=10
w/h
x/a
0.08
0.06
0.04
0.02
0
0.1
0.2
0.3
0.4
0.5
0.6
0.7
0.8
0.9
1

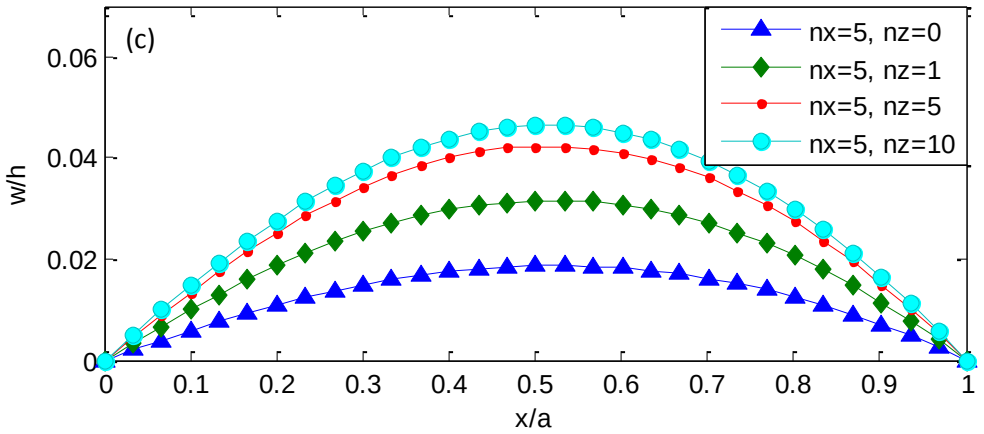
(c)
nx=5, nz=0
nx=5, nz=1
nx=5, nz=5
nx=5, nz=10
w/h
x/a
0.06
0.04
0.02
0
0.1
0.2
0.3
0.4
0.5
0.6
0.7
0.8
0.9
1

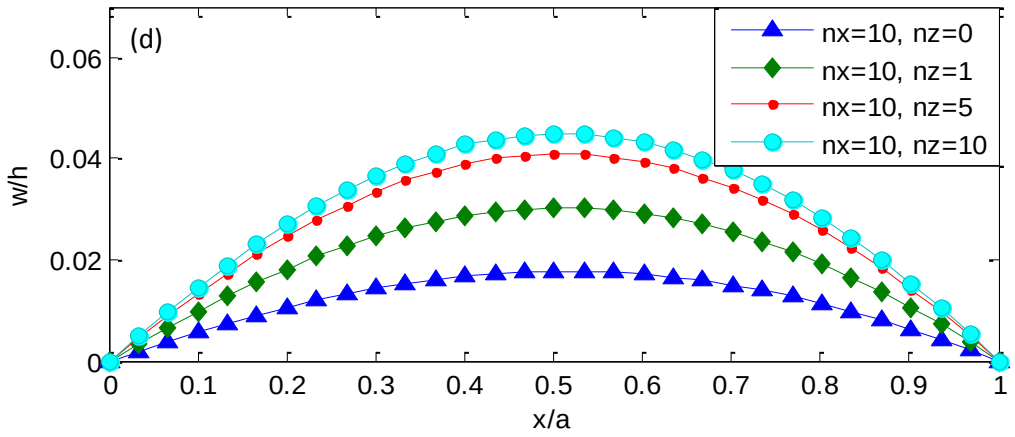

Figure 5. (a)-(d) Effects of material distribution on the change of dimensionless deflection during longitudinal middle line of fully simply supported cylindrical panels with various magnitudes of the power-law indices.

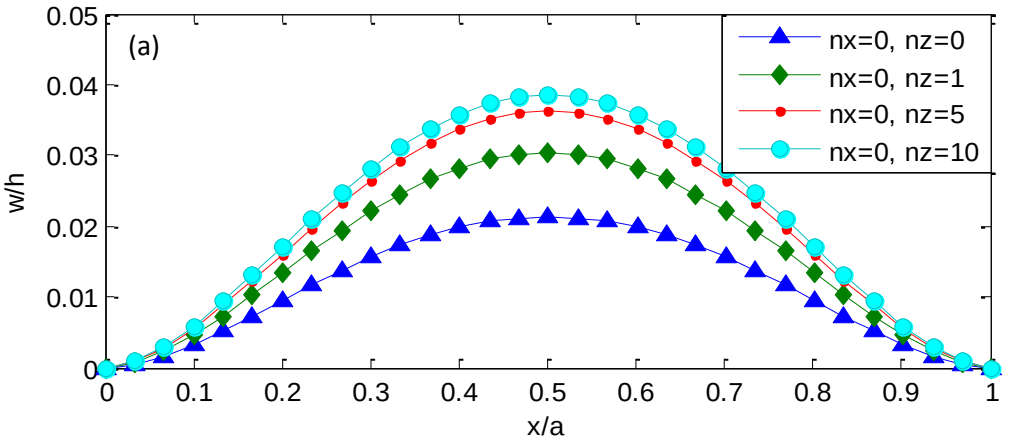

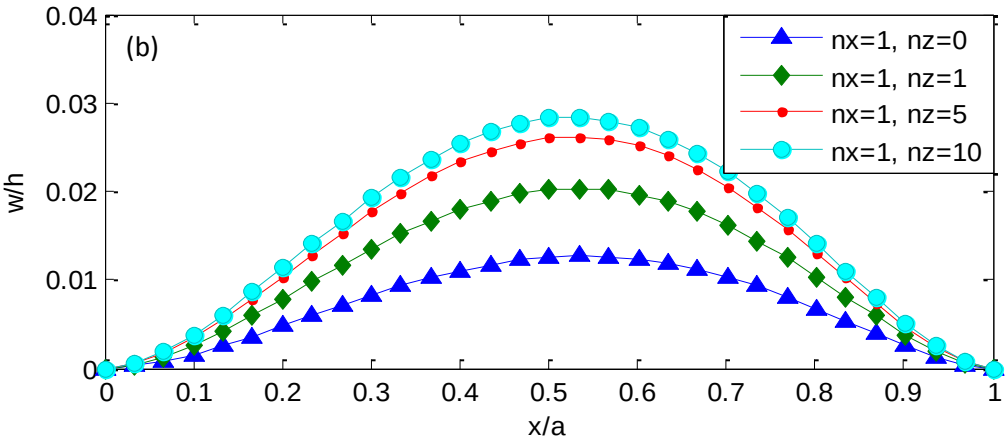

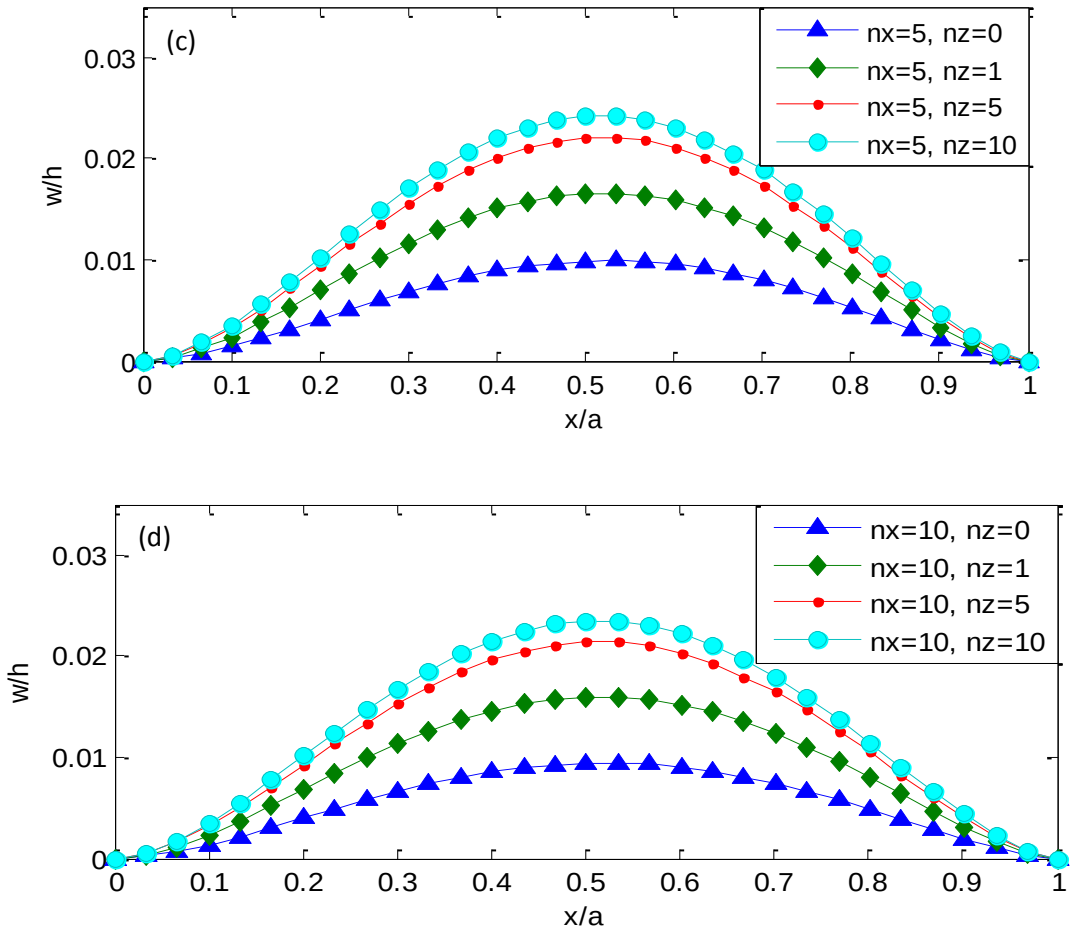

Figure 6. (a)-(d) Effects of material distribution on the change of dimensionless deflection during longitudinal middle line of CSCS cylindrical panels with various magnitudes of the power-law indices.

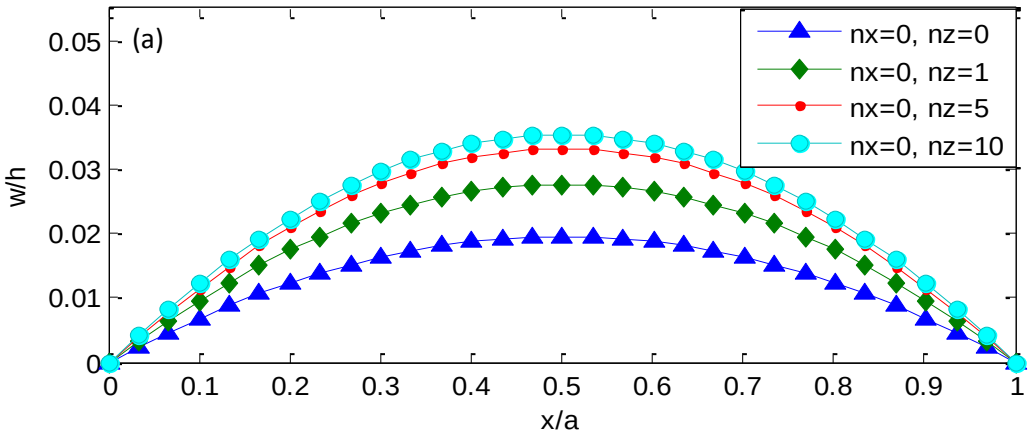

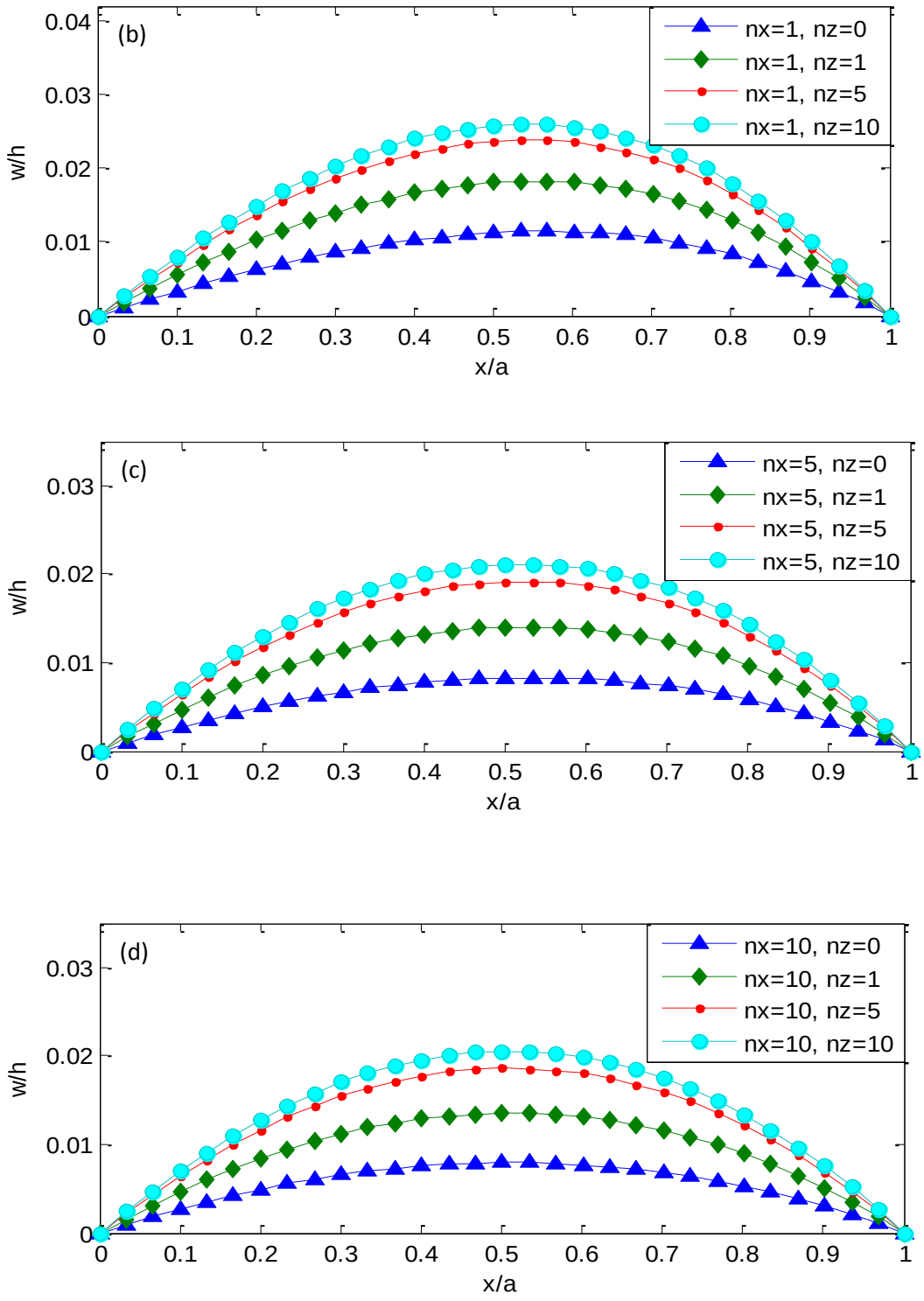

Figure 7. (a)-(d) Effects of material distribution on the change of dimensionless deflection during longitudinal middle line of SCSC cylindrical panels with various magnitudes of the power-law indices.

The effects of geometrical parameters on the change of dimensionless deflection during longitudinal middle line of 2-D FG cylindrical panels with various boundary conditions are shown in Figs. 8, 9 and 10. Fig. 8 shows the effect of radius R = 2, 1, 0.5, 0.25 and $\theta_0 = 5.73^o, 11.46^o, 22.92^o, 45.84^o$ on the change of dimensionless deflection during longitudinal middle line of 2-D FG cylindrical panels subjected to uniform load $P_z a^4/E_{m2}h^4 = 2.285715$ with (CCCC, SSSS) boundary conditions; respectively. It can be seen from Fig. 8 that with given power-law indices (nx = 2, nz = 2), the dimensionless deflection along longitudinal centerline of panel increases as the curvature to thickness (R/h) increases for various boundary conditions.

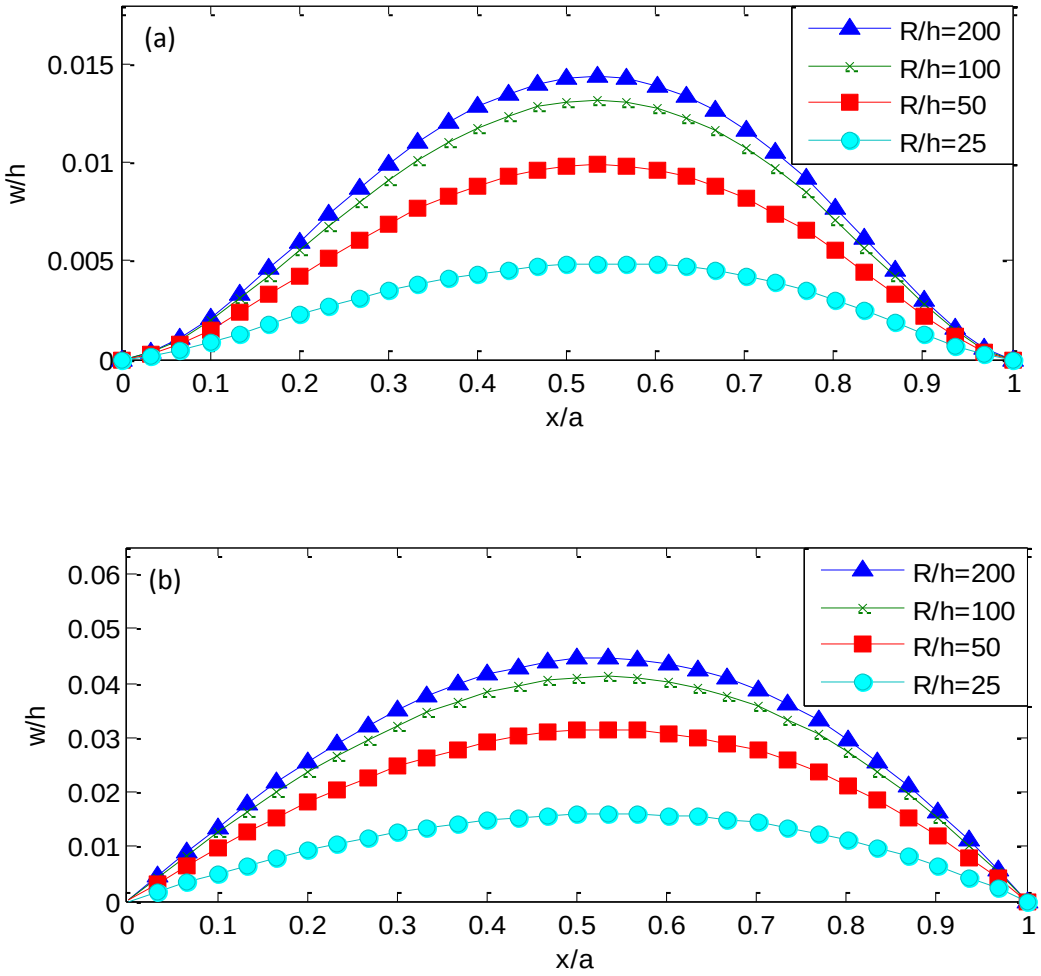

Figure 8. (a)-(b) Effects radius to thickness (R/h) ratio on dimensionless deflection during longitudinal middle line of 2-D FG cylindrical panels with (CCCC, SSSS) boundary conditions; respectively.

Fig. 9 represents the influence of thickness to radius ratio (h/R) on the dimensionless deflection during longitudinal middle line of 2-D FG cylindrical panels with various boundary conditions. The deflections are calculated for panels subjected to uniform load P_Z = 1MPa and has (R = 1, a = 0.2, b = 0.2) and h/R = 0.025, 0.02; respectively. It is observed that with particular power-law indices (nx = 3, nz = 3), the dimensionless deflection during longitudinal middle line of 2-D FG cylindrical panels increases as the thickness to radius ratio decreases.

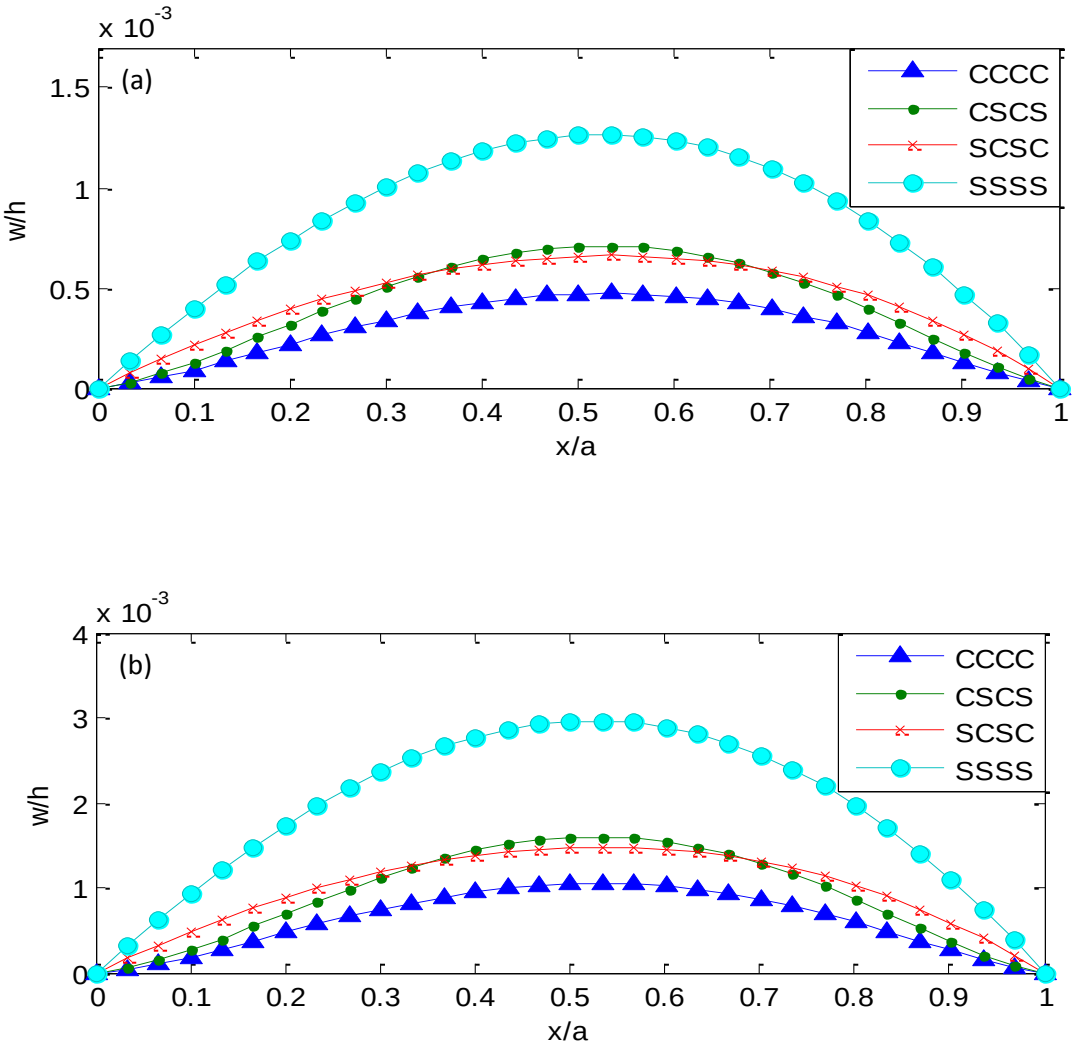

Figure 9. (a)-(b) Effects thickness ratio (h/R) on dimensionless deflection during longitudinal middle line of 2-D FG cylindrical panels with various boundary conditions for (h/R) = 0.025, 0.02; respectively.

Fig. 10 shows the change of dimensionless deflection along longitudinal centerline due to uniformly applied load P_Z = 1MPa, vs. dimensionless length a/h for fully clamped and fully simply supported cylindrical panels respectively. It is shown that for a/h = 10, 20, 30 and with particular power-law indices (nx = 3, nz = 3), the variation of the dimensionless deflection along longitudinal centerline increases as the length to thickness ratio increases. The increase in dimensionless deflections is explained beyond to around a/h = 10, under this the variation of non-dimensional deflections is very small.

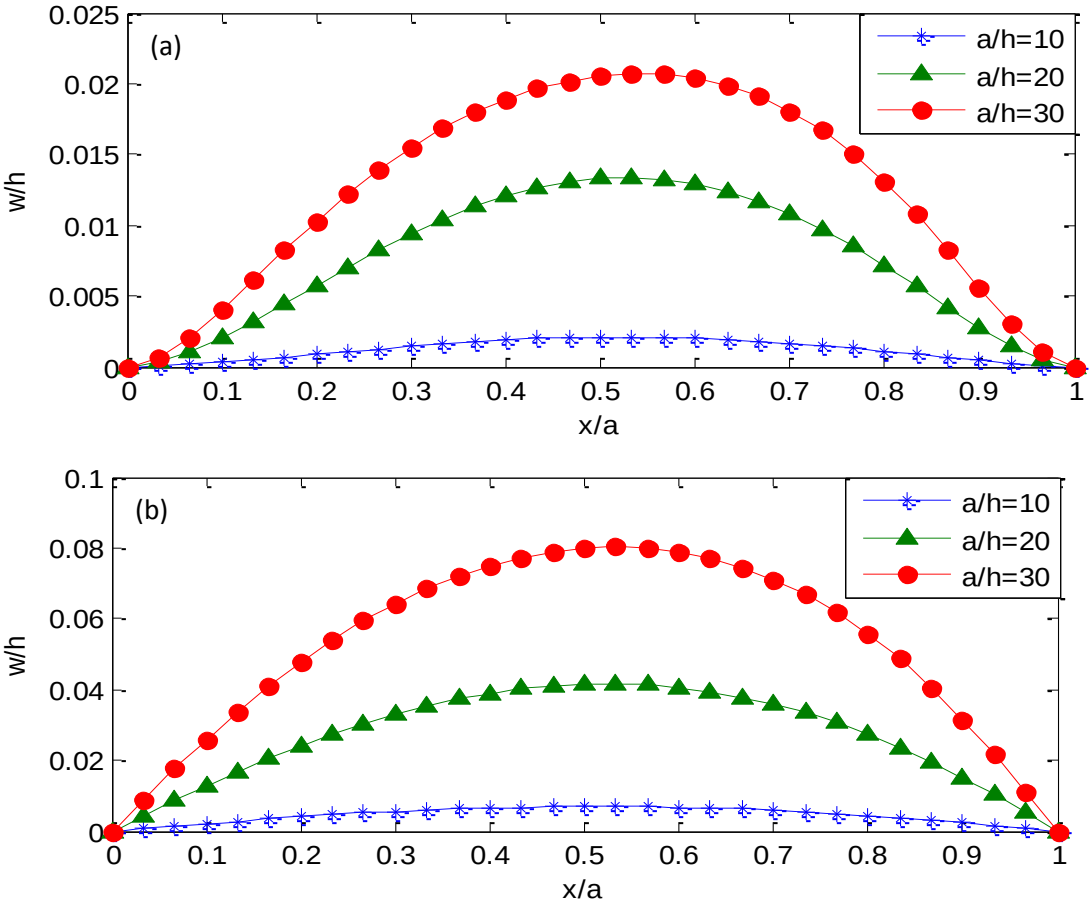

Figure 10. (a)-(b) Effects length to thickness (a/h) ratio on dimensionless deflection during longitudinal middle line of 2-D FG cylindrical panels with CCCC, SSSS boundary conditions; respectively.

7. Conclusions

Some universal views are explained as follows:

[1] Predictions of the FSDT for deflections of fully clamped plates using generalized differential quadrature (GDQ) method are approximately the same as those obtained utilizing the finite element method (FEM).

[2] The dimensionless deflections through longitudinal centerline increases with the increase in power-law index in thickness direction nz and decreases with the increase power-law index in longitudinal direction nx, for various boundary conditions.

[3] The influences of the value and style of the deflections depends on power-law index in longitudinal direction nx, but power-law index in thickness direction nz only effects on the value of the deflections.

[4] For various boundary conditions, the dimensionless deflections along longitudinal centerline increases as the radius to thickness (R/h) ratio increases.

[5] The magnitudes of dimensionless deflections during longitudinal middle line with fully simply supported are greater than fully clamped boundary condition and (CSCS, SCSC) between them.

[6] In small deflection range, cylindrical panels with simply supported edges is unsuitable in linear results.

[7] The dimensionless deflection of the panel enhances as the thickness ratio (h/R) increases for various boundary conditions.

[8] The non-dimensional deflections along longitudinal centerline increases with increase length to thickness (a/h) ratio for a/h = 20, 30 and becomes approximately

unresponsive to a/h ratio smaller than or equal 10.

References

[1] Koizumi M. The concept of FGM. Ceram Trans Funct Gradient Mater 1993;34:3-10.

[2] Holt JB. Functionally gradient materials. American Ceramic Society; 1993.

[3] Miyamoto Y, Kaysser W, Rabin B, Kawasaki A, Ford R. Functionally graded materials: design, processing and applications. Boston: Kluwer Academic Publishers; 1999.

[4] Nemat-Alla M, Ahmed KIE, Hassab-Alla I. Elastic-plastic analysis of two-dimensional functionally graded materials under thermal loading. Int J Solids Struct 2009;46(14-15):2774-86.

[5] Nie G, Zhong Z. Axisymmetric bending of two-directional functionally graded circular and annular plates. Acta Mech Solida Sin 2007;20(4):289-95.

[6] Asemi K, Salehi M, Akhlaghi M. Three dimensional static analysis of two dimensional functionally graded plates. IJMECH 2013;2(2):21-32.

[7] Alinaghizadeh F, Shariati M. Geometrically non-linear bending analysis of two-directional functionally graded annular sector and rectangular plates with variable thickness resting on non-linear elastic foundation. Compos Part B 2016;86:61-83.

[8] Basset AB. On the extension and flexure of cylindrical and spherical thin elastic shells. Philos Trans Roy Soc Lon Part A 1990;181:433-80.

[9] Horgan CO, Chan AM. The pressurized hollow cylinder or disk problem for functionally graded isotropic linear elastic materials. J Elast 1999;55(1):43-59.

[10] Shen HS, Noda N. Postbuckling of FGM cylindrical shells under combined axial and radial mechanical loads in thermal environments. Int J Solids Struct 2005;42(16-17):4641-62.

[11] Zhao X, Lee YY, Liew KM. Thermoelastic and vibration analysis of functionally graded cylindrical shells. Int J Mech Sci 2009;51(9-10):694-707.

[12] Sobhani Aragh B, Yas MH. Static and free vibration analyses of continuously graded fiber reinforced cylindrical shells using generalized power law distribution. Acta Mech 2010;215(1-4):155-73.

[13] Sobhani Aragh B, Yas MH. Three dimensional analysis of thermal stresses in four parameter continuous grading fiber reinforced cylindrical panels. Int J Mech Sci 2010;52(8):1047-63.

[14] Alibeigloo A. Thermoelastic solution for static deformations of functionally graded cylindrical shell bonded to thin piezoelectric layers. Compos Struct 2011;93(2):961-72.

[15] Alibeigloo A, Nouri V. Static analysis of functionally graded cylindrical shell with piezoelectric layers using differential quadrature method. Compos Struct 2010;9(8):1775-85.

[16] Liew KM, Kitipornchai S, Zhang XZ, Lim CW. Analysis of thermal stress behavior of functionally graded hollow circular cylinders. Int J Solids Struct 2003;40(10):2355-80.

[17] Viola E, Rossetti L, Fantuzzi N. Numerical investigation of functionally graded cylindrical shells and panels using the generalized unconstrained third order theory coupled with the stress recovery. Compos Struct 2012;94:3736-3758.

[18] Viola E, Rossetti L, Fantuzzi N, Tornabene F. Static analysis of functionally graded conical shells and panels using the generalized unconstrained third order theory coupled with the stress recovery. Compos Struct 2014;112:44-65.

[19] Aghdam MM, Shahmansouri N, Bigdeli K. Bending analysis of moderately thick functionally graded conical panels. Compos Struct 2011;93:1376-84.

[20] Rossetti L, Fantuzzi N, Viola E. Stress and displacement recovery for functionally graded conical shells. In: International conference on mechanics of nano, micro and macro composite structures, Torino; June 2012.

[21] Nemat-Alla M. Reduction of thermal stresses by developing two-dimensional functionally graded materials. Int J Solids Struct 2003;40(26):7339-56.

[22] Sobhani Aragh B, Hedayati H. Static response and free vibration of two-dimensional functionally graded metal/ceramic open cylindrical shells under various boundary conditions. Acta Mech 2012;223(2):309-30.

[23] Ebrahimi MJ, Najafizadeh MM. Free vibration analysis of two-dimensional functionally graded cylindrical shells. Appl Math Model 2014;38(1):308-24.

[24] Asgari M, Akhlaghi M. Transient thermal stresses in two-dimensional functionally graded thick hollow cylinder with finite length. Archiv Appl Mech 2010;80(4):353-76.

[25] Najibi A, Talebitooti R. Nonlinear transient thermo-elastic analysis of a 2D-FGM thick hollow finite length cylinder. Compos Part B 2017;111:211-227.

[26] Sanders JR. An improved first order approximation theory for thin shells. NASA technical report; 1959. R24.

[27] Reddy JN. Introduction to the finite element method. New York: McGraw-Hill;1993.

[28] Reddy JN. Energy principles and variational methods in applied mechanics. New York: John Wiley and Sons Inc; 1984.

[29] Saada AS. Elasticity: theory and applications. New York: Pergamon Press Inc.;1974.